

Fig. 5.15. Ensemble of models found during the search for acceptable models, using the method of Farmer (2000). The models are projected onto six pairs of parameter axes, and each plot range encompasses the entire parameter space. The dots are coloured by misfit, as indicated by the scale, and the acceptable models are coloured black.

A method for mapping the region of acceptable models found by the NA has been developed by Farmer (2000). This method attempts to map the complete range of models which satisfactorily fit the data, by transforming the data misfit criterion in order to concentrate sampling in and around the region of acceptable models. The actual misfit of an acceptable model is ignored, so that the probability of further sampling in its Voronoi cell (neighbourhood) is the same as for any other acceptable model. Thus all acceptable models are treated equally by the NA. Transforming the data misfit criterion to find acceptable models using the NA is discussed further in Sambridge (2001). Obviously some measure of whether a model is acceptable or not is needed, and this is represented by a certain misfit cut-off value.

As a result of collaborative work with Catherine Farmer this method was applied to the NA waveform inversion for source parameters. In the following we describe the method and provide an illustration for the southern Xinjiang event. The first step is to extract the acceptable models from the complete set of models generated during

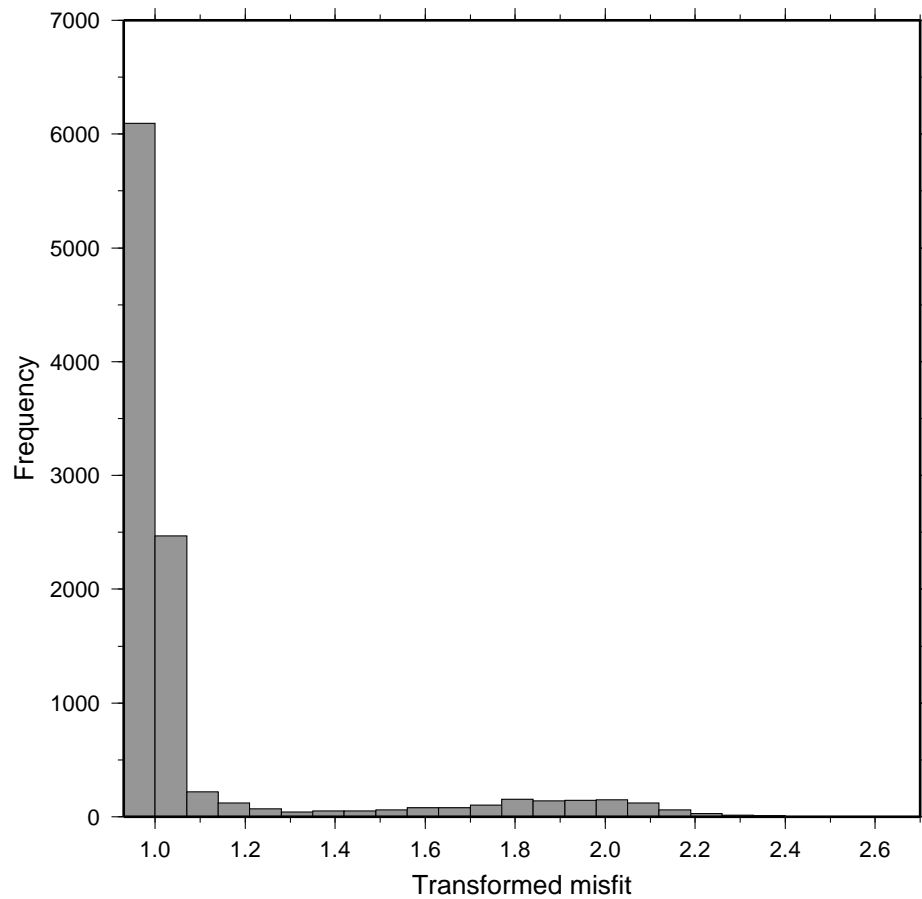


Fig. 5.16. Histogram of the transformed misfit values for the 10250 models found during the search for acceptable models, using the method of Farmer (2000). The acceptable models are those with a transformed misfit value of 1.0, and we can clearly see that the sampling is concentrated in and around the region of acceptable models.

the NA waveform inversion. By visual inspection of seismogram fits we decided that models with a misfit value of less than 0.17 are acceptable. Thus from the set of models plotted in Figure 5.13 we extract the models with misfit below the chosen misfit cut-off value of 0.17. This initial set of 108 acceptable models is then thinned by 4/5 in order to produce a more uniform initial sample, so that we are able to map the full extent of the acceptable region (see Farmer, 2000 for further details). Further models are generated randomly and added to the set of acceptable models, in order to obtain a reasonable initial sampling of the parameter space. This starting ensemble is then used to initiate the search for acceptable models with a transformed data misfit criterion. We note that subsequent work has revealed that it is not necessary to use a starting ensemble which includes acceptable models, instead it is possible to use a purely random set of models to initiate the inversion. The data misfit criterion was

transformed in the following way. All models with a misfit below the misfit cut-off (i.e. the acceptable models) were assigned a misfit value of 1.0, and all models with misfit above the misfit cut-off were assigned a scaled misfit value which was greater than 1.0. In this way the NA does not distinguish between acceptable models as they have equal misfit, and the sampling is concentrated in the cells bordering the region of acceptable models enabling the mapping of this region. An initial set of 250 models made up of 22 acceptable models and 228 randomly generated models is used. The Voronoi cells of the 200 highest ranked models are resampled, generating 200 new models at each iteration. The algorithm proceeds for 50 iterations.

The complete ensemble of models generated by applying this approach to the southern Xinjiang event is displayed in Figure 5.15. Again, each plot represents the projection of the ensemble of models onto a two-dimensional plane, and the colour scale represents misfit. In this case black represents the acceptable models, i.e. those with a transformed misfit value of 1.0. A comparison between Figure 5.15 and Figure 5.13 reveals that a much improved sampling of the entire parameter space is obtained, and in particular the region surrounding the acceptable models is well sampled. This is also illustrated in Figure 5.16 which shows a histogram of the misfit values for all the models generated during the search for acceptable models. It is clear that the sampling is concentrated in and around the region of acceptable models, with 6095 out of the 10250 models having a transformed misfit value of 1.0. We obtain a fairly small, well defined region of acceptable models (Figure 5.15) which indicates that the model parameters are well constrained, and that the best fitting model has small uncertainty associated with it. Obviously this will depend on the misfit cut-off used; if a higher misfit value is chosen the region of acceptable models will be larger. Due to the improved sampling of the parameter space, we can now clearly see evidence for a trade-off between the length of the source time function and depth in Figure 5.15. As mentioned earlier we might expect to see two minima in the fault plane parameters associated with the fault and auxiliary planes, however, there is no evidence for this in Figure 5.15. Farmer (2000) noted that if the depth and source time function are held fixed in the inversion, the two minima associated with the fault and auxiliary planes become apparent.

5.4 Kyrgyzstan event

We perform inversion for an event which occurred in Kyrgyzstan on 9 January 1997 (Figure 5.17). This event has an estimated m_b of 5.7, with a CMT depth estimate of 15 km. Thus we can again compare our inversion results with the CMT solution for

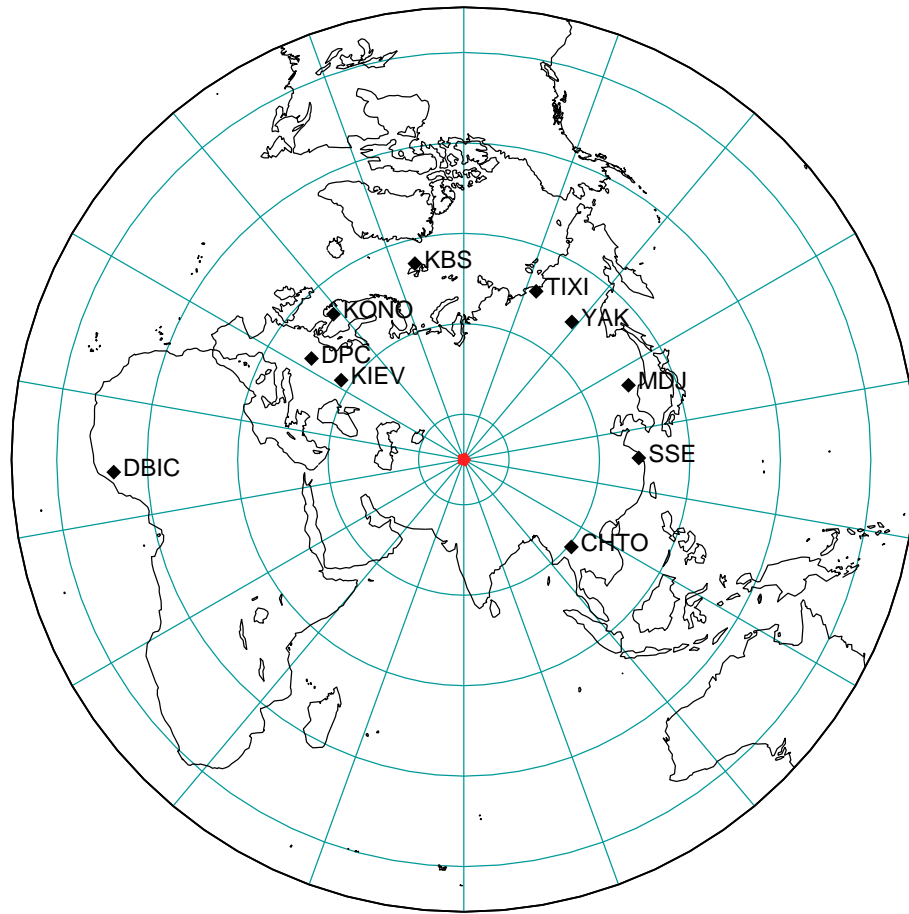


Fig. 5.17. Location of the 9 January 1997 Kyrgyzstan event along with the stations used in the inversion.

this event (Dziewonski et al., 1998). The waveforms used in the inversion have been obtained from the IRIS DMC. Ten stations are used in the inversion, but only four of the stations have suitable SV and SH waveforms due to low signal to P coda ratios for S . The waveforms are bandpass filtered in the range 0.01 Hz to 0.6 Hz before inversion.

We perform a joint P and S inversion, with a suitable weighting factor applied to the S wave data due to differing amounts of P and S information available. A moment tensor representation of the source mechanism is used, and we search over a wide range of source depths from 0 km to 35 km. We obtain a depth estimate of 15 km, which agrees with the CMT depth estimate. A reasonable fit to the observed seismograms is obtained for both P and S (Figure 5.18), though there are noticeable discrepancies at some stations (such as CHTO). This is probably due to the presence of complicated receiver structure beneath these stations. A comparison between the source mechanism estimates obtained from the NA inversion and the CMT inversion is shown in Figure 5.19. There is fairly good correspondence between the source

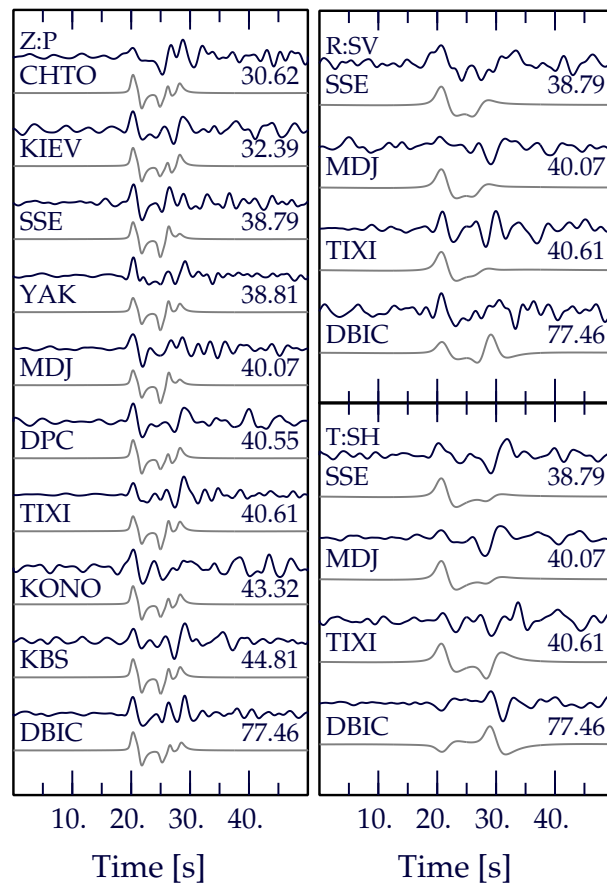


Fig. 5.18. Comparison between the observed (black traces) and predicted (grey traces) seismograms for the Kyrgyzstan event. Shown are the vertical component of P , and the radial and transverse components of S . Each set of traces is annotated with the station name and epicentral distance.

mechanism estimates, particularly for the P radiation pattern in the areas which are well sampled. The correspondence is not as good for SV and SH due to there being only four stations with suitable S waveforms, resulting in poor coverage of the S radiation patterns. We do not apply any constraints to the isotropic component of the moment tensor and obtain a small, but negligible, explosive component.

5.5 Indian nuclear test

As a test of the discrimination capabilities of our inversion method we perform inversion for a known nuclear explosion; the Indian nuclear test of 11 May 1998 (Figure 5.20). The USGS reported a m_b of 5.2 for this explosion, which implies an approximate yield of 10-15 kt (Wallace, 1998). The waveforms used in the inversion are obtained from the IRIS DMC. We found only six stations in the teleseismic distance range with good P wave signals (Figure 5.20). We would not expect to observe any SH wave energy,